HHS Public Access

Author manuscript

Biochem J. Author manuscript; available in PMC 2016 April 25.

Published in final edited form as:

Biochem J. 2015 February 15; 466(1): 123–135. doi:10.1042/BJ20140935.

Raptor ablation in skeletal muscle decreases Cav1.1 expression and affects the function of the excitation–contraction coupling supramolecular complex

Rubén J. Lopez[*], **Barbara Mosca**[*,†], **Susan Treves**[*,†], **Marcin Maj**[*], **Leda Bergamelli**[†], **Juan C. Calderon**[‡], **C. Florian Bentzinger**[§], **Klaas Romanino**[§], **Michael N. Hall**[§], **Markus A. Rüegg**[§], **Osvaldo Delbono**[‖], **Carlo Caputo**[‡], and **Francesco Zorzato**[*,†,1]

[*]Departments of Anesthesia and of Biomedicine, Basel University Hospital, Hebelstrasse 20, 4031 Basel, Switzerland [†]Department of Life Sciences, General Pathology section, University of Ferrara, Via Borsari 46, 44100 Ferrara, Italy [‡]Laboratorio de Fisiología Celular, Centro de Biofísica y Bioquímica, Instituto Venezolano de Investigaciones Científicas (IVIC), Apartado 20632, 1020A Caracas, Venezuela [§]Biozentrum, University of Basel, CH-4056 Basel, Switzerland [‖]Department of Internal Medicine, Section on Gerontology and Geriatric Medicine, Wake Forest University School of Medicine, Winston-Salem, NC 27157, U.S.A

Abstract

The protein mammalian target of rapamycin (mTOR) is a serine/threonine kinase regulating a number of biochemical pathways controlling cell growth. mTOR exists in two complexes termed mTORC1 and mTORC2. Regulatory associated protein of mTOR (raptor) is associated with mTORC1 and is essential for its function. Ablation of raptor in skeletal muscle results in several phenotypic changes including decreased life expectancy, increased glycogen deposits and alterations of the twitch kinetics of slow fibres. In the present paper, we show that in muscle-specific raptor knockout (RamKO), the bulk of glycogen phosphorylase (GP) is mainly associated in its cAMP-non-stimulated form with sarcoplasmic reticulum (SR) membranes. In addition, ^{3}[H]–ryanodine and ^{3}[H]–PN200-110 equilibrium binding show a ryanodine to dihydropyridine receptors (DHPRs) ratio of 0.79 and 1.35 for wild-type (WT) and raptor KO skeletal muscle membranes respectively. Peak amplitude and time to peak of the global calcium transients evoked by supramaximal field stimulation were not different between WT and raptor KO. However, the increase in the voltage sensor-uncoupled RyRs leads to an increase of both frequency and mass of elementary calcium release events (ECRE) induced by hyper-osmotic shock in flexor digitorum brevis (FDB) fibres from raptor KO. The present study shows that the protein composition and function of the molecular machinery involved in skeletal muscle excitation–contraction (E–C) coupling is affected by mTORC1 signalling.

[1]To whom correspondence should be addressed (zor@unife.it).

AUTHOR CONTRIBUTION

Ruben Lopez, Marcin Maj, Barbara Mosca, Leda Bergamelli and Susan Treves performed the experiments, analysed the data and drafted the article. Juan Calderon and Carlo Caputo critically revised the manuscript for important intellectual content. Osvaldo Delbono provided the plasmid with the $Ca_V1.1$ promoter. Florian Bentzinger, Klaas Romanino, Michael Hall and Markus Rüegg provided the muscle-specific Raptor knockout mouse. Francesco Zorzato designed and performed experiments, collection, analysis and interpretation of data and drafted the article.

Keywords

dihydropyridine receptor (DHPR); excitation–contraction (E–C); coupling; mammalian target of rapamycin (mTOR); ryanodine receptor (RyR); skeletal muscle sarcoplasmic reticulum (SR)

INTRODUCTION

The mammalian target of rapamycin (mTOR) is a serine/threonine kinase controlling different biochemical pathways activated in response to growth factors and nutrient availability, including protein synthesis, ribosome biogenesis, nutrient transport, lipid synthesis and autophagy, thus playing a central role in metabolism, growth and aging [1–5]. Two different mTOR complexes possessing different roles within the cell have been identified: mTORC1 and mTORC2. The immunosuppressant drug rapamycin is an allosteric inhibitor of mTORC1, a complex playing a role in nutrient sensing and controlling protein synthesis, lipid synthesis and glycolysis [6]. After forming a complex with its cytoplasmic receptor FKBP12 (FK506-binding protein), rapamycin binds mTORC1 and induces its destabilization, resulting in the inability of mTOR to phosphorylate target proteins [6]. mTORC1 complex is made up of mTOR, regulatory associated protein of mTOR (raptor), mammalian lethal with SEC13 protein 8/G-protein β-subunit like protein (mLST8/GβL) and proline-rich Akt substrate of 40 kDa (PRAS40) [7,8]. Its kinase activity is regulated through a dynamic interaction between mTOR and raptor, the latter being a conserved 150 kDa protein, which besides mTOR, also interacts with S6K1 (ribosomal protein S6 kinase 1) and 4E–BP1 (eukaryotic translation initiator factor 4E-binding protein 1). mTORC2 on the other hand, is largely insensitive to rapamycin, is active in growing cells and regulates the actin cytoskeleton, cell survival and apoptosis. It forms a complex with rictor, mSIN1 (target of rapamicin complex 2 subunit Mitogen-activated protein kinase 2-associated protein 1), mLST8 and mTOR [9].

During the past decade, research on the role of mTOR has revealed that this kinase is implicated in a variety of diseases, including cancer, neurodegeneration and metabolic disorders [9]. Furthermore mTOR activity has been shown to be involved in the control of muscle mass and indeed rapamycin treatment delays recovery of skeletal muscle from atrophy whereas activation of the mTOR's upstream components induces muscle hypertorphy [10]. It has been shown that skeletal muscle-specific mTOR inactivation increases the glycogen content of muscle fibres, an effect linked to the down-regulation of glycogen phosphorylase (GP) and of other enzymes involved in the glycogenolytic pathway [11]. Similar results were also obtained by Bentzinger et al. [12] who investigated the role of the mTORC1 signalling pathway in skeletal muscle, by generating muscle-specific raptor knockout mice (RamKO). Skeletal muscles of RamKO mice became progressively atrophic, had increased glycogen content and showed a transition of the metabolic signature from oxidative to glycolitic, despite slow twitch fibre-type predominance [12]. Although RamKO mice have poor *in vivo* oxidative muscle performance on the running wheel, *in vitro* tetanic stimulation shows that isolated extensor digitorum longus (EDL) and soleus from RamKO mice are more resistant to fatigue. The reduction in absolute force development is accounted for by the decrease in muscle mass, since after normalization for cross-sectional area (CSA)

there is no significant difference in maximal tetanic force between control and RamKO mice. Nevertheless the twitch kinetics of the soleus from RamKO mice is dramatically affected: there is an increased time to peak and almost doubling of the half relaxation time. Because of these changes and because mTORC1 inhibition is a common therapeutic strategy in humans, we investigated in more detail the functional changes of ablation of mTORC1 in skeletal muscle by examining excitation–contraction (E–C) coupling in RamKO mice. E–C coupling involves the conversion of an electrical signal into a transient increase in the intracellular [Ca^{2+}] and is initiated by conformational changes at the level of the L-type voltage-dependent calcium channel [dihydropyridine receptor (DHPR), $Ca_v1.1$] localized in the membrane of the transverse tubules [13,14]. Activation of Ca^{2+} release from terminal cisternae is due to the transmission of a conformational change occurring on the DHPR to the ryanodine receptor (RyR)1 via direct protein–protein interaction [15–17]. The resulting increase in the intracellular [Ca^{2+}] is due to the opening of the RyR1 and this is followed by Ca^{2+} removal, which depends mostly on the activity of sarcoplasmic reticulum (SR) calcium pumps (SERCA) localized in the longitudinal SR and, to a lesser extent, on the sarcolemmal Na^+/Ca^{2+} exchanger and plasmalemma Ca^{2+} pump [18]. Mutations in the two Ca^{2+} channels (RyR1 and DHPR α1 subunit) directly involved in E–C coupling are the underlying feature of a group of several disorders including core myopathies in which the underlying histological feature is the presence of cores and fibre type I pre-dominance (for review see [19]). Interestingly, the muscles of RamKO mice also exhibit core-like structures and slow fibre-type predominance [12].

In the present study, we investigated the functional and biochemical properties of the SR membranes from RamKO mice. We found that the inactivation of mTORC1 is associated with the compartmentalization of GP to SR membranes. In addition, we found an increase in the: (i) half-time of the decay of the calcium transient in soleus fibres; (ii) ryanodine to DHPRs ratio; (iii) frequency and mass of elementary calcium release events (ECRE) induced by hyperosmotic shock in FDB fibres. Altogether our data suggest that protein composition and function of the membrane compartments involved in E–C coupling is affected by mTORC1 signalling.

MATERIALS AND METHODS

RamKO mice

Details of the targeting strategy and initial characterization of RamKO mice are previously described [12]. KO mice were identified by PCR amplification of genomic DNA. All experiments were conducted on male mice in accordance with local Kantonal guidelines and regulations (Kantonales Veterinäramt Basel Stadt).

RNA extraction, reverse transcription and PCR reactions

Total RNA was extracted from mouse leg muscles using Tri-reagent following the manufacturer's recommendations (Molecular Research Centre). Total RNA was converted into cDNA using SuperScript™ II Reverse Transcriptase (Invitrogen) as previously described [20]. PCR reactions were carried out using the following primer sets: mouse β-actin forward: 5′-GGACCTGACAGACTACCTCA-3′ and reverse 5′-

GCAGTAATCTCCTTCTGCAT-3′; DHPRα1 ($Ca_v1.1$) forward 5′-CATTAGGTAGAGCCGTGCACCTG-3′ and reverse 5′-GCCTGTTGTCATGACGAAGTTAGC-3′. Amplification conditions were 5 min at 95°C followed by 35 cycles of 30 s denaturation at 92°C, 40 s annealing at the recommended temperature for each primer pair and 40 s extension at 72°C followed by a final extension for 5 min at 72°C using the 2.5× Master Mix Taq polymerase from Eppendorf. The products of the PCR reaction were separated on a 1% agarose gel and the DNA bands were visualized by Ethidium Bromide staining.

SR isolation, Western blotting and biochemical assays

Total SR was prepared as previously described from mouse skeletal muscle [20]; vesicles enriched in terminal cisteranae, longitudinal SR and plasmalemma were prepared as described by Saito et al. [21] and stored in liquid nitrogen until used. C_2C_{12} myotubes were treated for 16 h with 20 μM rapamycin or left untreated; cells were then washed twice with PBS, harvested, and the heavy SR protein fraction was obtained by differential centrifugation. For Western blotting, proteins were separated by SDS/PAGE, blotted on to nitrocellulose and probed with commercial antibodies (Abs) against SR proteins [SERCA1, SERCA 2, calsequestrin, calreticulin (CR), sarcalumenin, RyR1, DHPRα1, DHPR β1, albumin, SRP-35 (SR protein of 35 kDa) or anti-JP-45 Abs; 20]) followed by peroxidase-conjugated secondary Abs. The immunopositive bands were visualized by chemiluminescence as previously described [22]. To accurately quantify DHPR and RyR content in the SR and the Ca^{2+} dependency of [^{3}H]-ryanodine binding, radioligand-binding experiments using [^{3}H]-PN200-110 (DHPR expression) and [^{3}H]-ryanodine were performed as described [23]. The different free [Ca^{2+}] (750 pM, 9.1 nM, 95 nM, 1.1 μM, 9 μM, 104 μM, 1 mM) were obtained by the addition of different amounts of $CaCl_2$ as described by Fabiato [24]. The amount of bound [^{3}H] ligand was measured by liquid scintillation counting.

In vitro muscle strength assessment

To test force *in vitro*, EDL and soleus muscles were dissected and mounted into a muscle-testing setup (Heidelberg Scientific Instruments). Muscles were stimulated with 15-V pulses for 0.5 ms and force was digitized at 4 kHz by using an AD instruments converter. EDL tetanus was recorded in response to a 400 ms train of pulses delivered at 10–120 Hz; soleus tetanus was recorded in response to an 1100 ms train of pulses delivered at 10–150 Hz. Specific force was normalized to the muscle CSA per wet weight (mg)/length (mm) per 1.06 (density mg/mm^3) as previously described [23].

Isolation of extensor digitorum longus and soleus muscle fibres

Single muscle fibres were obtained from 6–8 week old mouse hindlimbs by enzymatic dissociated, as previously described [25]. Briefly, muscles were dissected and pinned via the tendons to a Sylgard-lined dissecting chamber. The outer connective tissue was removed and the muscles were incubated in Tyrode's solution containing 0.22% type I collagenase (Sigma) at 37°C for 1 h followed by rinsing in 10% fetal bovine serum (FBS) in DMEM (Dulbecco's Modified Eagle's medium). To release single fibres, muscles were triturated gently in serum-free DMEM, then plated on glass coverslips pre-treated for 2 h with 1.5 μl

of natural mouse laminin (Invitrogen) diluted with distilled water. Fibres were then incubated in DMEM, 10% FBS, 1% penicillin/streptomycin, 5% CO_2 at 37°C overnight. FDB fibres were isolated as previously described [23].

Calcium measurements

The resting [Ca^{2+}] was monitored in isolated fibres from RamKO mice and control littermates with the ratiometric fluorescent Ca^{2+}-indicator indo-1/AM (acetoxymethylesther); changes in the $[Ca^{2+}]_i$ induced by electrical depolarization were monitored in EDL and soleus fibres loaded with mag–fluo–4/AM in Tyrode's buffer. All experiments were carried out at room temperature (20°C–22°C) in the presence of 50 μM *N*-benzyl-*p*-toluensulfonamide (BTS; Tocris) to minimize movement artefacts. Measurements were carried out with a Nikon ECLIPSE TE2000-U inverted fluorescent microscope equipped with a 20× PH1 DL magnification objective. The light signals from a spot of 1 mm diameter of the magnified image of flexor digitorum brevis (FDB) fibres, were converted into electrical signals by a photomultiplier connected to a Nikon Photometer P101 amplifier. Calcium transients were collected by custom made (RCS AUTOLAB) software and analysed by PowerLab Chart5 and Origin.6 programs. Changes in fluorescence were calculated as $\Delta F/F = (F_{max} - F_{rest})/(F_{rest})$.

FDB fibres were isolated, kept for 4 h in a 37°C, 5% CO_2 cell incubator, placed on a laminin-coated coverslip and loaded for 20 min at room temperature with 10 μM fluo-4 AM Ca^{2+} indicator (fluo-4/AM, Molecular Probes). All experiments were performed at room temperature. ECREs were measured using a Nikon A1R laser scanning confocal microscope (Nikon Instruments Inc.) with a 60× oil immersion Plan Apo VC Nikon objective, numerical aperture 1.4. (Nikon Instruments Inc.). Five-second-duration linescan images (*x,t*) were acquired in resonant mode at 7680 lps with 512 pixels (0.05 μm/pixel) in the *x*- and 39936 pixels (0.126 ms/pixel) in the *t*-direction using a pinhole size of 72.27 μm. Fifteen images were taken at different positions across each cell. The Ca^{2+} indicator was excited with a laser at 487 nm and the fluorescence emitted at 525 ± 25 nm was recorded. To minimize photo damage, the laser intensity was set at 3%–4% of the maximal power. The viability of fibres after osmotic shock was assessed by monitoring single calcium transient evoked by supramaximal field stimulation pulses. Fibres were first perfused with isotonic (~290 mOsm) normal Ringer (NR) (in mM, 140 NaCl; 2 $MgCl_2$; 2.5 $CaCl_2$; 10 HEPES; 5 KCl; pH adjusted to 7.4) using a Minipuls 2 peristaltic pump (Gilson Medical Electronics). To induce ECREs, cells were perfused with a hypertonic solution (~420 mOsm) by increasing the [Ca^{2+}] to 50 mM (in mM, 140 NaCl; 2 $MgCl_2$; 50 $CaCl_2$; 10 HEPES; 5 KCl; pH adjusted to 7.4) [26,27]. Osmolarity of the solution was assessed with a Vogel 801 Osmometer (Vogel GmbH). All solution contained 10 μM BTS.

ECRE analysis

ECREs morphology [amplitude, $\Delta F/F_0$; full width at half-maximum amplitude (FWHM); full duration at half-maximum amplitude (FDHM)] were determined from linescan images using the open source image analyser software Fiji [28]. After images were binned by average 4× at the *t*-axis, they were processed using the automated spark detection plugin Sparkmaster [29]. Because of the heterogeneity of the ECREs duration, events were split in

two groups: the short lasting events with <50 ms of FWHM and the long lasting events ECREs with >50 ms of FWHM duration [30]. Frequency was calculated for each group by counting the number of events occurring per image. The mass was determined by the following formula mass= $1.206 \cdot \Delta F/F_0 \cdot \mathrm{FWHM}^3$ [31]. Statistical analysis was performed using the program OriginPro® version 8.6.0. ECRE derived from 25 and 26 fibres obtained from five wild-type (WT) and RamKO mice respectively. Data are expressed as mean ± S.E.M.; values were considered statistically significant if $P < 0.05$ using the Student's *t*-test.

Glycogen phosphorylase activity measurement

GP activity was measured as described [32–34]. Reactions were initiated by adding 30–60 μg of SR to a 500 μl of reaction buffer containing 50 mM imidazole pH 7.0, 20 mM K_2HPO_4, 1.25 mM $MgCl_2$, 5 μM glucose 1,6-diphosphate, 0.5 mM DTT, 3 μg/ml phosphoglucomutase, 0.25% BSA, 10 mg/ml AMP-free glycogen. For measurement of total activity (forms 'a' and 'b' of GP) AMP was added to obtain a final concentration of 3 mmol/l. The reaction was carried out at 30°C for 30 min (total activity) or for 60 min (to determine the amount of form 'a') and terminated by the addition of 60 μl of 0.5 M HCl. Aliquots of 50 or 100 μl (for total and form 'a' measurement respectively) of primary reaction mixture were added to 1 ml of a glucose-6-phosphate dehydrogenase reaction buffer containing 50 mM Tris/HCl, pH 8.0, 1 mM EDTA, 250 μM NADP and 0.5 μg/ml glucose-6-phosphate dehydrogenase. This reaction was allowed to proceed for 10 min at room temperature and the absorbance of the samples at 340 nm was determined spectrophotometrically to quantify the degree of conversion of NADP into NADPH (which is proportional to the content of glucose 6-phosphate formed in the first reaction). GP activity is expressed in micromoles per minute per milligram protein (unit/mg).

Luciferase reporter assay

The constructs containing DHPRα 1.1 promoter region fragments (Luc7P–724, Luc/P756) were cloned in frame in pGL3-basic expression vector (Promega) [35]. C_2C_{12} myoblasts (2×10^4 cells per dish) were plated on gelatin-coated 35 mm cell culture dishes and allowed to grow in DMEM plus Glutamax, 4.5 g/l glucose, 20% FBS, 50 units/ml penicillin, 50 μg/ml streptomycin until 50% confluent. Two microgram of each construct and 200 ng of the control vector pRL–TK were used for transfection using the FuGENE6 transfection reagent (Roche). Twenty-four hours after transfection, cells were induced to differentiate by changing the medium to DMEM plus Glutamax, 4.5 g/l glucose, 5% horse serum and penicillin/streptomycin. After 4–6 days, when cells had visibly fused into mytoubes, 20 μM rapamycin (Sigma) was added as described [36,37]. Cells were then washed twice with PBS and lysed using Passive Lysis Buffer (Promega). Firefly luciferase and renilla activity were measured with Victor^2 Luminometer (PerkinElmer). Firefly luciferase activity was normalized to renilla activity and expressed as mean (± S.E.M.) enzymatic activity units.

RESULTS

Mechanical properties of isolated fibres and content of proteins involved in excitation–contraction coupling in skeletal muscles of RamKO mice

Ablation of raptor induces changes in the mechanical properties of fast and slow twitch muscles [12]; Figure 1 shows representative traces of twitch and tetanic force of EDL and soleus from control and RamKO mice [12]. Although tetanic-specific force in EDL and soleus muscles do not vary between control and RamKO [12] mice, the twitch kinetics in RamKO soleus show a remarkable prolongation of the half relaxation time at lower peak force. The changes of the mechanical properties of the twitch in EDL and soleus muscles could be due (i) to fibre-type switching induced by ablation of raptor, (ii) to an effect on the contractile protein machinery, (iii) to alterations of the E–C coupling mechanism or (iv) to a combination of two or more of these mechanisms.

Protein composition of skeletal muscle sarcoplasmic reticulum from RamKO mice

Analysis of the main protein components of total SR membranes from RamKO mice and control littermates revealed no significant changes in the content of SERCA1, SERCA2, JP-45, calsequestrin and CR. In addition, there was a small but significant decrease in sarcalumenin (Figure 2), a modulator of SERCA activity [38]. We also found a decrease in SRP-35, a newly identified membrane-bound retinol dehydrogenase of sarcotubular membranes [22].

RamKO ablation affects the excitation–contraction coupling macromolecular complex

To study in greater detail the effect of raptor ablation, we determined the membrane density of the two core components of the E–C coupling machinery, namely the $Ca_v1.1$ ($\alpha 1.1$ of the DHPR) and RyR1 by performing quantitative Western blot analysis and equilibrium ligand binding on the crude microsomal preparation isolated from skeletal muscle of RamKO and control littermates. The most interesting results of the present study are that the content of $Ca_v1.1$ in RamKO mice was reduced by almost 50% compared with control littermates (Figure 3A). Equilibrium binding of the $Ca_v1.1$ ligand PN200-100 to crude SR membranes shows that the maximal binding capacity (B_{max}) for PN200-100 binding was 0.68 ± 0.05 and 1.25 ± 0.13 pmol/mg protein in RamKO and control littermates respectively with no significant changes of its dissociation constant (K_d = 0.96 ± 0.16 compared with 1.35±0.32 nM, mean ±S.E.M., n=6 for RamKO and control littermates respectively). The reduced expression of $Ca_v1.1$ is, surprisingly, accompanied by a 3.5-fold increase in the content of the $Ca_v\beta 1$ subunit (Figures 3B and 3C). On the other hand, the decrease in the total amount of $Ca_v1.1$ was not due to a reduction in the relative amount in T-tubule membranes in the total sarcotubular membrane fraction, as the content of albumin, a marker for T-tubules [39] was unchanged (Figures 3B, 3C and 4B). mTORC1 regulates protein expression by affecting translation via S6K1 and 4E–BP [5] and/or by controlling the transcription of several additional genes [40]. To determine if the decrease in $Ca_v1.1$ in the muscles of RamKO mice was due to alterations in transcription we performed semi-quantitative PCR experiments. As shown in Figure 4(A), there were no significant changes in $Ca_v1.1$ mRNA content in RamKO mice. We next evaluated the activity of the $Ca_v1.1$ promoter in C_2C_{12} myotubes and human embryonic kidney (HEK)293 cells transfected with a luciferase reporter construct

containing the 5′ flanking region of the $Ca_v1.1$ gene. Figure 4(C) shows that the $Ca_v1.1$ promoter is active in C_2C_{12} myotubes but not in HEK293 cells. Since FKBP12 is a ubiquitously expressed protein, including in C_2C_{12} myotubes [41], we next tested the effect of rapamycin, a drug which pharmacologically mimics the effect of knocking out raptor, on the activity of the Ca_v 1.1 promoter. Incubation of C_2C_{12} myotubes for 2 and 16 h with 20 μM rapamycin abolished the phosphorylation of the mTORC1 downstream target S6 ribosomal protein (Figure 4D), without influencing the activity of the Ca_v 1.1 promoter (Figure 4C). Nevertheless, rapamycin treatment of C_2C_{12} myotubes causes a decrease in the immunoreactive band corresponding to the $Ca_v1.1$ (Figure 4E) without effecting CR content, an extrinsic protein of the SR membrane. Our data clearly show that, even in the presence of a partial inhibition of the mTORC1 complex [42], the phenotype of rapamycintreated C_2C_{12} cells recapitulates the effect of $Ca_v1.1$ expression observed in RamKO mature skeletal muscle fibres. In particular, it appears that functional ablation of mTORC1 affects the synthesis and/or the stability of $Ca_v1.1$. A great deal of data show that rapamycin dissociates FKBP12 from the RyR complex, leading to leaky RyRs [43]. It is unlikely that the decrease in the Cav1.1 expression results from the acute appearance of leaky RyR in C_2C_{12} cells, since chronic disregulation of intracellular calcium concentration in muscle fibres expressing leaky RyR1 mutation do not display a decrease in $Ca_v1.1$ current density [44]. The decrease in the total sarcotubular membrane density of $Ca_v1.1$ was apparently also not paralleled by a decrease in the SR RyR1 calcium release channels, as we found no change in the B_{max} of equilibrium [^{3}H]ryanodine binding to the total SR membrane fraction (0.99+/−0.10 compared with 0.92+/−0.07 pmol/mg protein for WTand RamKO respectively) (Figure5)from RamKO and control littermates.

Glycogen phosphorylase is targeted to sarcoplasmic reticulum membrane in skeletal muscle from RamKO mice

Skeletal muscles from RamKO and control littermates were homogenized and fractionated by differential centrifugation. Comparison with the protein profile of total homogenates shows a decrease in a band of 97 kDa in the total homogenate of skeletal muscle from RamKO mice compared with that from control littermates (Figure 6A,*). It was previously shown that skeletal-muscle-specific mTORC1 inactivation reduces the content of GP, a result consistent with glycogen accumulation in RamKO muscle fibres [11,12]. Nevertheless, SDS gel electrophoresis of isolated SR membrane fractions revealed that the band with an apparent molecular mass of 97 kDa was enriched in the total SR of RamKO mice (Figure 6A, **). MS identified the 97 kDa SR protein band as the GP. This finding was further confirmed by staining a Western blot of total SR membrane proteins with specific anti-GP Abs (Figure 6D). Quantification showed that ablation of raptor led to a 2.9-fold increase in GP associated with the total SR membrane fraction (Figure 6B). Sub-fractionation of SR membranes by sucrose density centrifugation revealed that GP was enriched in the light R1 fraction (Figure 6C; white arrowheads), which is made up of membranes derived from longitudinal SR, sarcolemma and T-tubules. GP activity is regulated in several ways including (i) substrate availability, (ii) interconversion (phosphorylation/dephosphorylation), and (iii) allosteric modification, with AMP being a key activator [45,46]. We assessed whether the cAMP-stimulated (GP-a) or cAMP non-stimulated (GP-b) forms of the enzyme are enriched in the muscle from RamKO mice. As

shown in Figure 6(E), there was a similar increase in GP-total and GP-b activity, suggesting that the cyclic AMP-non-stimulated form of GP is enriched in the SR membranes of RamKO mice [47]. Hirata et al. reported that GP is a negative regulator of RyR since it decreases mastoparan-induced calcium release [48] and thus may affect the twitch kinetics. To explore this possibility, we studied Ca^{2+} homoeostasis in enzymatically-dissociated single EDL and soleus fibres.

Calcium transients on isolated EDL and soleus fibres

To assess the resting calcium concentration, we loaded EDL and soleus fibres with the ratiometric fluorescent Ca^{2+} indicator Indo-1. In both WT and RamKO mice, the resting [Ca^{2+}] in EDL fibres from control mice is slightly higher compared with that in soleus fibres. On the other hand, EDL and soleus fibres from RamKO mice exhibited a small but significant decrease in the resting [Ca^{2+}] compared with control littermates (Table 1). Mag–fluo–4, a low affinity calcium indicator, was used to monitor rapid Ca^{2+} transients (Figure 7) elicited by an action potential in single EDL and soleus fibres excited by supramaximal field stimulation [49]. The results we obtained are summarized in Table 1. The $\Delta F/F$ peak Ca^{2+} transient amplitude in EDL from WT (0.46 ± 0.04, mean ± S.E.M. n = 29 fibres) mice was 18% and 22% higher compared with that of soleus muscles from WT (0.38 ± 0.02, mean ± S.E.M., n = 22 fibres) and RamKO (0.36 ± 0.02, mean ± S.E.M. n = 5 fibres) mice respectively. Surprisingly, the peak amplitude and the 10%–90% rise time of the calcium transients were not different between RamKO mice and control littermates both in EDL and in soleus. The 10%–90% fall time of the calcium transients in soleus from RamKO mice is increased compared with that of WT (120.2 ± 15.7, n = 25 compared with 66.2 ± 7.4, n = 22 fibres respectively; values are mean ± S.E.M.; P<0.05 Mann Whitney test). The 10%–90% fall time of the calcium transients reflects the removal of calcium from the cytosol leading to muscle relaxation. Slow fibres are distinct from fast fibres since they typically display a lower relaxation rate compared with fast fibres [50]. In addition, peak calcium release induced by an action potential is lower in slow fibres compared with fast fibres [51]. The increase in 10%–90% fall time and the decrease in $\Delta F/F$ peak Ca^{2+} transient are consistent with the observation that almost 100% of the fibres of the soleus from RamKO mice are of type 1 [12]. EDL fibres from RamKO mice exhibited a small and non-significant increase in 10%–90% fall time of the calcium transients. Similar results were also obtained with enzymatically-dissociated FDB fibres (result not shown).

The lack of a decrease in the peak amplitude calcium transients evoked by an action potential in RamKO EDL and soleus fibres is apparently inconsistent with the decrease in density of $Ca_v1.1$ in the T-tubular membrane. A number of possibilities may account for this discrepancy. For example, the 50% decrease in Ca_v 1.1 in RamKO fibres ought to be accompanied by a larger fraction of voltage-sensor uncoupled RyR1. It has been proposed that (i) the interaction of $Ca_v1.1$ with RyR1 inhibits the appearance of ECRE in mammalian adult muscle fibres [26,50,52] and that (ii) the global calcium transients supporting E–C coupling in skeletal muscle fibres may result from the summation of ECRE [30]. Equilibrium binding on total microsomes shows that in RamKO there are five/six uncoupled RyRs per voltage-sensor coupled RyR, whereas in WT there is one/two uncoupled RyR per voltage-sensor-coupled RyR. On the basis of the equilibrium ligand-binding data, we

reasoned that the doubling of the voltage-sensor-uncoupled RyRs may affect ECRE. If this were so, the release of calcium from voltage-coupled RyRs in RamKO fibres might propagate to adjacent voltage-sensor-uncoupled RyRs triggering a larger number of ECRE, which together contribute to the global amplitude of the peak calcium transients in muscle fibres from RamKO. In the next set of experiments, we set out to test this idea by measuring the ECRE properties in FDB fibres from WT and RamKO mice induced by hyperosmotic shock [26,27], a treatment that weakens the inhibitory activity of $Cav_{1.1}$ on the RyR1 and thus unmasks the spontaneous activity of RyR1.

Elementary calcium release events in WT and RamKO FDB fibres

Intact single FDB fibres from WT and RamKO mice were first perfused with NR solution and then they were exposed to hyperosmotic Ringer solution containing 50 mM $CaCl_2$ [26,27]. After exposure to hyperosmotic solution, the FDB fibres were rinsed with NR and their viability was confirmed by their ability to respond with a robust global calcium transient upon the delivery of an action potential by supramaximal field stimulation (Supplementary Figure S1). The perfusion of FDB fibres from WT and RamKO with NR solution did not cause the appearance of spontaneous ECRE (Figures 8A, 8C, 8D and 8F left panels). Exposure to hyperosmotic Ringer solution solution containing 50 mM $CaCl_2$ [26,27], induced localized increase in fluo-4 fluorescence signals, which were mostly distributed under the inner leaflet of the sarcolemma (Figures 8B and 8E, Supplementary videos). Reperfusion of FDB fibres with NR abolished the appearance of local transient increases in fluo-4 fluorescence (Figures 8C and 8F). Figures 8(H) and 8(I) show *x,t* line scan images of fibre exposed to hyperosmotic solution. As can be seen, hyperosmotic treatment causes a transient increase in the fluorescence and, on the basis of the criteria proposed by Kirsch et al. [30], we refer to the local increase in fluo–4 fluorescence as ECRE. ECRE analysis was performed with Sparkmaster plug-in and ECRE were divided into two groups: short-lasting (sparks-like) events having a FDHM lower than 50 ms and long-lasting (ember-like) events with FDHM higher than 50 ms [29]. Analysis of 1923 and 2547 short-lasting ECRE from WT and RamKO fibres revealed significant differences of the morphological parameters of ECRE (Table 2). Although the amplitude of short-lasting ECRE was not different between WT and RamKO FDB fibres, the latter fibres exhibited a 10% increase in both FWHM (0.89 ± 0.01 compared with 0.98 ± 0.01 μm for WT and RamKO FDB fibres respectively; $P < 0.05$) and FDHM (13.31 ± 0.26 compared with 14.11 ± 0.24 ms for WT and RamKO FDB fibres respectively; $P < 0.05$). The estimated ECRE mass at peak time of the $\Delta F/F$ was 37% increased in RamKO FDB fibres (0.62 ± 0.02 compared with 0.85 ±0.03 μm^3 for WT and RamKO FDB fibres respectively; $P < 0.05$). The increase in estimated ECRE mass was paralleled by a 30% increase in the frequency of short lasting ECRE events in RamKO fibre (6.81 ±0.36 compared with 8.83 ±0.40 sparks/image for WT and RamKO FDB fibres respectively; $P < 0.05$). The appearance of ECRE in both WT and RamKO fibres dropped to zero upon pre-incubation of the fibres with RyR, indicating that the calcium source flux of ECRE are the RyR calcium release channels (Figures 8J and 8K).

DISCUSSION

In the present study, we investigated the structural and functional properties of the membrane compartment involved in E–C coupling of skeletal muscle from WT and raptor KO mice. Our results show that muscle-specific ablation of raptor, and the consequent down-regulation of the mTORC1 complex, causes a 1.70-fold increase in the RyR1 to DHPRs ratio in total sarcotubular membranes. This event increases both the frequency and the width of ECRE induced by exposure of FDB fibres to hyperosmotic shock. In addition, in RamKO skeletal muscles, the cAMP non-stimulated form b of GP is mostly associated with the sarcotubular membrane fraction. We propose that mTORC1 signalling affects the structure and function of the membrane compartments involved in E–C and excitation–glycogen metabolism coupling.

$Ca_V1.1$ content in RamKO mice

The transmission of the signal from the T-tubular membrane to the SR is performed by a supramolecular complex in the contact region between the two membrane systems. The core components of such a complex are the α_1-subunit ($Ca_V1.1$) of the L-type Ca^{2+} channel DHPR, the RyR and calsequestrin which serve as voltage sensor, SR Ca^{2+} release channel and calcium storage protein respectively [13]. The decrease in the membrane density of DHPR is not accompanied by a decrease in the membrane density of the RyR1 whereby the ryanodine to DHPRs ratio of RamKO mice is higher compared with that of WT mice. The lower membrane density of the DHPR is neither due to mis-localization of the protein to a different membrane compartment as the total amount of $Ca_V1.1$ was also reduced in the total muscle homogenate, nor to decreased levels of specific transcript. A similar decrease in the membrane density of DHPR was previously reported by Avila and Dirksen [37] upon acute treatment of cultured myotubes with 20 μM rapamycin and confirmed in the present study in C_2C_{12} cells treated in culture with rapamycin. However, it seems that the functional effect caused by the decreased membrane density of DHPR depends on the maturation stage of muscle cells, namely in myotubes [37] it causes a substantial decrease in the voltage-dependent calcium release, whereas in mature RamKO FDB fibres (in the present work) calcium release evoked by action potential is not affected. The decrease in DHPR content may be caused by increased degradation via ubiquitination and indeed it has been shown that rapamycin treatment induces protein ubiquitination in rat myocardium and mTOR inhibition induces autophagy [53,54]. Interestingly, the ratio of DHPR to RyR1 in slow fibres is lower compared with that in fast fibres, leading to a higher content of uncoupled RyR1 in soleus compared with fast twitch muscles [55]. Thus, our equilibrium binding results are consistent with the fast to slow fibre transition in RamKO muscles [12], in particular more than 90% of soleus's fibres from RamKO are of type 1. Importantly, however, although this reduction in voltage sensor does not seem to be directly responsible for changes in E–C coupling, it may trigger some of the structural variations seen in biopsied muscles, particularly the presence of smaller fibres containing core-like structures such as those described in the mouse RamKO muscles [12]. Indeed, immunofluorescence analysis of skeletal muscle biopsies from some patients with recessive *RYR1* mutations show that mis-alignment of RyR1 and DHPR is a feature of some patients with core myopathies [56]. A decrease in the DHPR calcium channels has also been reported in myotubular/centronuclear myopathy [57,58].

Razidlo et al. [59] proposed that the lack of myotubularin inhibits Akt signalling to mTORC1 leading to down-regulation of the signalling pathways mediated by the mTORC1 complex.

RyR/$Ca_V1.1$ ratio in skeletal muscle of RamKO mice

High resolution EM has demonstrated that $Ca_V1.1$ are organized in groups made up of four units regularly oriented in the T-tubular membrane to form structures referred to as tetrads, which correspond to the position of every other RyR localized in the opposite SR terminal cisternae membrane [14]. Equilibrium binding with total sarcotubular membrane fractions shows a ryanodine to DHPR ratio of 0.79 and 1.35 for WT and RamKO skeletal muscle respectively. The RyR/DHPR ratio we found in WT is consistent with that found by others in total rabbit skeletal muscle homogenates and total microsomal fraction [60–62]. Assuming that there are four PN200-110 binding sites per tetrad and one ryanodine-binding site per RyR, these results imply that in sarcotubular membranes from RamKO mice there is one tetrad-coupled RyR every five/six RyRs, whereas in WT sarcotubular membranes there is one tetrad-coupled RyR every 2–3 RyRs. The ryanodine to DHPR ratio of skeletal muscle from RamKO mice is more similar to that of cardiac [60] and or amphibian [61] skeletal muscles than to that of mature mammalian skeletal muscle. Thus, at this time, it is difficult to reconcile the functional behaviour of such a large fraction of uncoupled RyR in RamKO fibres with that of uncoupled RyR present in WT skeletal muscle having canonical ryanodine to DHPR ratios. Although a great deal of data do not support the notion that in mammalian skeletal muscle fibres, uncoupled RyR are activated by the calcium released from voltage-sensor coupled RyRs via calcium-induced calcium release [63–65], we cannot exclude the possibility that the large ‘cardiac-like’ fraction of voltage-sensor uncoupled RyR in RamKO fibres might have distinct functional behaviour.

Global calcium signals and elementary calcium release events in WT and RamKO fibres

Measurements of global calcium in single EDL, soleus and FDB show no differences in the peak amplitude of depolarization-induced Ca^{2+} release between WT and RamKO. Such a result was unexpected because of the significant decrease in the membrane density of DHPR and is not consistent with the general idea that the DHPR drives the voltage-dependent activation of RyR1. Nevertheless, it may be possible that a large fraction of uncoupled RyRs are sensitive to regulation by physiological modulators and the activation of the uncoupled RyRs might compensate for the lower content of voltage sensors in RamKO muscles. This line of reasoning is supported by our finding of the modification of the morphology of ECRE induced by osmotic shock, a manoeuvre which weakens the control of the DHPR over the RyR1 and may thus unmask a distinct regulatory mechanism of uncoupled RyR1 in RamKO fibres. ECRE in RamKO fibres are spatially wider and this apparently does not correlate with the changes of the amplitude of ECRE between WT and RamKO fibres. A larger FWHM of ECRE in FDB fibres from raptor KO mice may be caused by a decrease in the removal of calcium at the source site by SERCA and/or by cytosolic calcium-binding proteins. A decrease in removal of calcium is probably not due to the changes in the membrane density of the Ca^{2+} pump, since staining of Western blots with either SERCA1 or SERCA2 Ab did not reveal differences in their protein level in crude SR membrane preparations. The wider ECRE in RamKO fibres may result from the recruitment of the

larger fraction of RyRs which are not directly coupled to DHPRs, as described in frog skeletal muscles [65], a tissue with a ryanodine to DHPRs ratio higher than that of mammalian skeletal muscle fibres [61]. If such a distinct functional behaviour is also operating in RamKO skeletal muscle fibres under physiological condition, it is possible that during an action potential voltage-operated RyR1 channels open and the calcium released by the voltage-operated RyR1s propagates to neighbouring uncoupled RyR1 channels. The latter channels release calcium by a calcium-induced calcium release mechanism and ultimately contribute to the calcium transient.

Compartmentalization of glycogen phosphorylase to SR membrane

In skeletal muscle, glycogen forms a dense network of granules which are mostly localized on the myoplasmic surface of terminal cisternae and along the membrane of the fenestrated collar [66]. Excitation of skeletal muscle is associated by a rapid (seconds) glycogen breakdown via activation of GP, the enzyme responsible for the release of glucose-1-phosphate from glycogen particles, which ultimately supports muscle metabolism during exercise. It has been demonstrated that excitation–glycolysis coupling occurs without an increase in the myoplasmic concentration of cAMP and without the subsequent conversion of GP-b into GP-a by the cAMP-dependent activity of phosphorylase kinase [67]. GP-b can be allosterically activated by AMP; this cAMP-non-stimulated activity is thought to be predominant during the early phases of skeletal muscle contraction [68]. In resting conditions, the intracellular concentration of AMP is not sufficient to activate GP-b, thus GP-b is thought to be inactive in resting muscles [69]. During strenuous muscle activity however, the intracellular AMP concentration increases, signalling a demand in energy requirement. AMP is the product of the activity myokinase, an enzyme which utilizes as a substrate the ADP generated by the activity of the SR calcium ATPase (CaATPase), Na^+/K^+-ATPase and myosin-ATPase. In resting conditions, the average myoplasmic concentration of AMP is 0.2 μM and it increases 10-fold during intense muscle activity [70,71]. However, in regions of high ATP consumption, such as in domains where the SERCA enzyme pumps calcium back into the SR, a greater amount of ATP is required and this may be made available by the allosteric activation of GP-b by AMP. Interestingly, lower glycogen content and an increase in its degradation have been linked to a fast decay of calcium transients and force during tetanic stimulation [72,73]. The cAMP-dependent active form of GP-a inhibits the activation of the RyR1 by caffeine [48]. Thus, the presence of GP-b associated with the SR membrane is consistent with the concept that the increase in fatigue resistance described in RamKO [11] mice correlates with sustained calcium release, thanks to the compartmentalization to the SR of an energy supplying system made up of glycogen and GP-b.

Overall these results indicate that the muscle phenotype of RamKO mice is complex and due to the interaction of multiple biochemical pathways governed by the mTORC1 signalling complex. The present study shows that an adequate mTORC1 activity is required to maintain the structure and the function of the membrane compartments involved in E–C coupling.

Supplementary Material

Refer to Web version on PubMed Central for supplementary material.

Acknowledgments

We gratefully acknowledge Anne-Sylvie Monnet's technical support.

FUNDING

This work was supported by the Department of Anesthesia, Basel University Hospital, Telethon, Italy [grant number GGP14003].

Abbreviations

Ab	antibody
AM	acetoxymethylesther
BTS	*N*-benzyl-*p*-toluensulfonamide
CR	calreticulin
CSA	cross-sectional area
DHPR	dihydropyridine receptor
DMEM	Dulbecco's Modified Eagle's medium
E–C	excitation–contraction
ECRE	elementary calcium release events
EDL	extensor digitorum longus
FDB	flexor digitorum brevis
FDHM	full duration at half-maximum amplitude
FKBP12	FK506-binding protein
FWHM	full width at half-maximum amplitude
GP	glycogen phosphorylase
HEK	human embryonic kidney
KO	knockout
mLST8	mammalian lethal with SEC13 protein 8
mTOR	mammalian target of rapamycin
NR	normal Ringer
RamKO	muscle-specific raptor knockout
raptor	regulatory associated protein of mTOR
RyR	ryanodine receptor
SERCA	sarcoplasmic reticulum calcium pump

SR	sarcoplasmic reticulum
SRP-35	SR protein of 35 kDa
WT	wild-type

References

1. De Virgilio C, Loewith R. The TOR signalling network from yeast to man. Int J Biochem Cell Biol. 2006; 38:1476–1481. [PubMed: 16647875]
2. Wullschleger S, Loewith R, Hall MN. TOR signaling in growth and metabolism. Cell. 2006; 124:471–48. [PubMed: 16469695]
3. Guertin DA, Sabatini DM. Defining the role of mTOR in cancer. Cancer Cell. 2007; 12:9–2. [PubMed: 17613433]
4. Yang Q, Guan KL. Expanding mTOR signaling. Cell Res. 2007; 17:666–68. [PubMed: 17680028]
5. Hay N, Sonenberg N. Upstream and downstream of mTOR. Genes Dev. 2004; 18:1926–194. [PubMed: 15314020]
6. Banaszynski LA, Liu CW, Wandless TJ. Characterization of the FKBP rapamycin FRB ternary complex. J Am Chem Soc. 2006; 127:4715–4721. [PubMed: 15796538]
7. Kim DH, Sarbassov DD, Ali SM, King JE, Latek RR, Erdjument-Bromage H, Tempst P, Sabatini DM. mTOR interacts with raptor to form a nutrient-sensitive complex that signals to the cell growth machinery. Cell. 2002; 110:163–17. [PubMed: 12150925]
8. Kim DH, Sarbassov DD, Ali SM, Latek RR, Guntur KV, Erdjument-Bromage H, Tempst P, Sabatini DM. GbetaL, a positive regulator of the rapamycin-sensitive pathway required for the nutrient-sensitive interaction between raptor and mTOR. Mol Cell. 2003; 11:895–90. [PubMed: 12718876]
9. Dazert E, Hall MN. mTOR signalling in disease. Curr Opin Cell Biol. 2011; 23:705–70. [PubMed: 22018538]
10. Bodine SC, Stitt TN, Gonzalez M, Kline WO, Stover GL, Bauerlein R, Zlotchenko E, Scrimgeour A, Lawrence JC, Glass DJ, Yancopoulos GD. Akt/mTOR pathway is a crucial regulator of skeletal muscle hypertrophy and can prevent muscle atrophy *in vivo*. Nat Cell Biol. 2001; 3:1009–101. [PubMed: 11715022]
11. Risson V, Mazelin L, Roceri M, Sanchez H, Moncollin V, Corneloup C, Richard-Bulteau H, Vignaud A, Baas D, Defour A, et al. Muscle inactivation of mTOR causes metabolic and dystrophin defects leading to severe myopathy. J Cell Biol. 2009; 187:859–87. [PubMed: 20008564]
12. Bentzinger CF, Romanino K, Cloetta D, Lin S, Mascarenhas JB, Oliveri F, Xia J, Casanova E, Costa CF, Brink M, et al. Skeletal muscle-specific ablation of raptor, but not of rictor, causes metabolic changes and results in muscle dystrophy. Cell Metab. 2008; 8:411–42. [PubMed: 19046572]
13. Rios E, Pizarro G. Voltage sensor of excitation-contraction coupling in skeletal muscle. Physiol Rev. 1991; 71:849–908. [PubMed: 2057528]
14. Franzini-Armstrong C, Jorgensen AO. Structure and development of E–C coupling units in skeletal muscle. Annu Rev Physiol. 1994; 56:509–53. [PubMed: 8010750]
15. Beam KG, Tanabe T, Numa S. Structure, function, and regulation of the skeletal muscle dihydropyridine receptor. Ann N Y Acad Sci. 1989; 560:127–13. [PubMed: 2545129]
16. Schneider MF, Chandler WK. Voltage dependent charge movement of skeletal muscle: a possible step in excitation-contraction coupling. Nature. 1972; 242:244–246. [PubMed: 4540479]
17. Melzer W, Hermann-Frank A, Luttgau HC. The role of Ca^{2+} ions in excitation-contraction coupling of skeletal muscle fibres. Biochim Biophys Acta. 1995; 1241:59–11. [PubMed: 7742348]
18. Fleischer S, Inui M. Biochemistry and biophysics of excitation-contraction coupling. Annu Rev Biophys Biophys Chem. 1989; 18:333–36. [PubMed: 2660829]

19. Treves S, Jungbluth H, Muntoni F, Zorzato F. Congenital muscle disorders with cores: the ryanodine receptor calcium channel paradigm. Curr Opin Pharmacol. 2008; 8:319–32. [PubMed: 18313359]
20. Anderson AA, Treves S, Biral D, Betto R, Sandoná D, Ronjat M, Zorzato F. The novel skeletal muscle sarcoplasmic reticulum JP-45 protein: molecular cloning, tissue distribution, developmental expression and interaction with α.1 subunit of the voltage gated calcium channel. J Biol Chem. 2003; 278:39987–3999. [PubMed: 12871958]
21. Saito A, Seiler S, Chu A, Fleischer S. Preparation and morphology of sarcoplasmic reticulum terminal cisternae from rabbit skeletal muscle. J Cell Biol. 1984; 99:875–88. [PubMed: 6147356]
22. Treves S, Thurnheer R, Mosca B, Vukcevic M, Bergamelli L, Voltan R, Oberhauser V, Ronjat M, Csernoch L, Szentesi P, Zorzato F. SRP-35, a newly identified protein of the skeletal muscle sarcoplasmic reticulum, is a retinol dehydrogenase. Biochem J. 2012; 44:731–741. [PubMed: 21995425]
23. Delbono O, Xia J, Treves S, Wang ZM, Jimenez-Moreno R, Payne AM, Messi ML, Briguet A, Schaerer F, Nishi M, et al. Loss of skeletal muscle strength by ablation of the sarcoplasmic reticulum protein JP45. Proc Natl Acad Sci USA. 2007; 104:20108–2011. [PubMed: 18077436]
24. Fabiato A. Computer programs for calculating total from specified free or free from specified total ionic concentrations in aqueous solutions containing multiple metals and ligands. Methods Enzymol. 1988; 157:378–41. [PubMed: 3231093]
25. Calderon JC, Bolanos P, Caputo C. Myosin heavy chain isoform composition and Ca^{2+} transients in fibres from enzymatically dissociated murine soleus and extensor digitorum longus muscles. J Physiol. 2010; 588:267–279. [PubMed: 19884322]
26. Wang X, Weisleder N, Collet C, Zhou J, Chu Y, Hirata Y, Zhao X, Pan Z, Brotto M, Cheng H, Ma J. Uncontrolled calcium sparks act as a dystrophic signal for mammalian skeletal muscle. Nat Cell Biol. 2005; 7:525–53. [PubMed: 15834406]
27. Apostol S, Ursu D, Lehmann-Horn F, Melzer W. Local calcium signals induced by hyper-osmotic stress in mammalian skeletal muscle cells. J Muscle Res Cell Motil. 2009; 30:97–10. [PubMed: 19437123]
28. Schindelin J, Arganda-Carreras I, Frise E, Kaynig V, Longair M, Pietzsch T, Preibisch S, Rueden C, Saalfeld S, Schmid B, et al. Fiji: an open-source platform for biological-image analysis. Nat Methods. 2001; 9:676–682. [PubMed: 22743772]
29. Picht E, Zima AV, Blatter LA, Bers DM. SparkMaster: automated calcium spark analysis with ImageJ. Am J Physiol Cell Physiol. 2007; 293:C1073–C108. [PubMed: 17376815]
30. Kirsch WG, Uttenweiler D, Fink RH. Spark- and ember-like elementary Ca^{2+} release events in skinned fibres of adult mammalian skeletal muscle. J Physiol. 2001; 537:379–8. [PubMed: 11731572]
31. Hollingworth S, Peet J, Chandler WK, Baylor SM. Calcium sparks in intact skeletal muscle fibers of the frog. J Gen Physiol. 2001; 118:653–67. [PubMed: 11723160]
32. Danforth WH, Helmreich E, Coric F. The effect of contraction and of epinephrine on the phosphorylase activity of frog sartorius muscle. Proc Natl Acad Sci USA. 1962; 48:1191–119. [PubMed: 13883372]
33. Chasiotis D, Brandt R, Harris RC, Hultman E. Effects of beta-blockade on glycogen metabolism in human subjects during exercise. Am J Physiol. 1983; 245:E166–E170. [PubMed: 6309009]
34. Rush JW, Spriet LL. Skeletal muscle glycogen phosphorylase a kinetics: effects of adenine nucleotides and caffeine. J Appl Physiol. 2001; 91:2071–2078. [PubMed: 11641346]
35. Zheng Z, Wang ZM, Delbono O. Charge movement and transcription regulation of L-type calcium channel α_{1S} in skeletal muscle cells. J Physiol. 2002; 540:397–40. [PubMed: 11956331]
36. Lamb GD, Stephenson DG. Effects of FK506 and rapamycin on excitation-contraction coupling in skeletal muscle fibres of the rat. J Physiol. 1996; 494:569–57. [PubMed: 8842013]
37. Avila G, Dirksen RT. Rapamycin and FK506 reduce skeletal muscle voltage sensor expression and function. Cell Calcium. 2005; 38:35–4. [PubMed: 15955561]
38. Yoshida M, Minamisawa S, Shimura M, Komazak S, Kume H, Zhang M, Matsumura K, Nishi M, Saito M, Saeki Y, et al. Impaired Ca^{2+} store functions in skeletal and cardiac muscle from sarcalumenin-deficient mice. J Biol Chem. 2005; 280:3500–350. [PubMed: 15569689]

39. Knudson CM, Campbell KP. Albumin is a major protein component of transverse tubule vesicles isolated from skeletal muscle. J Biol Chem. 1989; 264:10795–10798. [PubMed: 2732247]
40. Peng T, Golub TR, Sabatini DM. The immunosuppressant rapamycin mimics a starvation-like signal distinct from amino acid and glucose deprivation. Mol Cell Biol. 2002; 22:5575–558. [PubMed: 12101249]
41. Shin DW, Pan Z, Bandyopadhyay A, Bhat MB, Kim DH, Ma J. Ca^{2+} -dependent interaction between FKBP12 and calcineurin regulates activity of the Ca^{2+} release channel in skeletal muscle. Biophys J. 2002; 83:2539–25492. [PubMed: 12414688]
42. Nyfeler B, Bergman P, Triantafellow E, Wilson CJ, Zhu Y, Radetich B, Finan PM, Klionsky DJ, Murphy LO. Relieving autophagy and 4EBP1 from rapamycin resistance. Mol Cell Biol. 2011; 31:2867–287. [PubMed: 21576371]
43. Andersson DC, Betzenhauser MJ, Reiken S, Meli AC, Umanskaya A, Xie W, Shiomi T, Zalk R, Lacampagne A, Marks AR. Ryanodine receptor oxidation causes intracellular calcium leak and muscle weakness in aging. Cell Metab. 2011; 14:196–20. [PubMed: 21803290]
44. Durham WJ, Aracena-Parks P, Long C, Rossi AE, Goonasekera SA, Boncompagni S, Galvan DL, Gilman CP, Baker MR, Shirokova N, et al. RyR1 S-nitrosylation underlies environmental heat stroke and sudden death in Y522S RyR1 knockin mice. Cell. 2008; 133:53–6. [PubMed: 18394989]
45. Cuenda A, Henao F, Nogues M, Gutierrez-Merino C. Quantification and removal of glycogen phosphorylase and other enzymes associated with sarcoplasmic reticulum membrane preparations. Biochim Biophys Acta. 1994; 1194:35–43. [PubMed: 8075139]
46. Johnson LN. Glycogen phosphorylase: control by phosphorylation and allosteric effectors. FASEB J. 1992; 6:2274–2282. [PubMed: 1544539]
47. Cuenda A, Nogues M, Henao F, Gutierrez-Merino C. Interaction between glycogen phosphorylase and sarcoplasmic reticulum membranes and its functional implications. J Biol Chem. 1995; 270:11998–1200. [PubMed: 7744850]
48. Hirata Y, Atsumi M, Ohizumi Y, Nakahata N. Mastoparan binds to glycogen phosphorylase to regulate sarcoplsmic reticulm Ca^{2+} release in skeletal muscle. Biochem J. 2003; 371:81–8. [PubMed: 12519071]
49. Hollingworth S, Gee KR, Baylor SM. Low-affinity Ca^{2+} indicators compared in measurements of skeletal muscle Ca^{2+} transients. Biophys J. 2009; 97:1864–187. [PubMed: 19804716]
50. Heizmann CW, Berchtold MW, Rowlerson AM. Correlation of parvalbumin concentration with relaxation speed in mammalian muscles. Proc Natl Acad Sci USA. 1982; 79:7243–724. [PubMed: 6961404]
51. Baylor SM, Hollingworth S. Intracellular calcium movements during excitation-contraction coupling in mammalian slow-twitch and fast-twitch muscle fibers. J Gen Physiol. 2012; 13:261–272. [PubMed: 22450485]
52. Zhou J, Yi J, Royer L, Launikonis BS, Gonzalez A, Garcia J, Rios E. A probably role of dihydropyridine receptors in repression of Ca^{2+} sparks demonstrated in cultured mammalian muscle. Am J Physiol Cell Physiol. 2006; 290:C539–C55. [PubMed: 16148029]
53. Jung CH, Ro SH, Cao J, Otto NM, Kim DH. mTOR regulation of autophagy. FEBS Lett. 2010; 584:1287–129. [PubMed: 20083114]
54. Harston RK, McKillop JC, Moschella PC, Van Laer A, Quinones LS, Baicu CF, Balasubramanian S, Zile MR, Kuppuswamy D. Rapamycin treatment augments both protein ubiquitination and Akt activation in pressure -overloaded rat myocardium. Am J Physiol Heart Circ Physiol. 2011; 300:H1696–H1706. [PubMed: 21357504]
55. Delbono O, Meissner G. Sarcoplasmic reticulum Ca^{2+} release in rat slow and fast-twitch muscles. J Membr Biol. 1996; 151:123–13. [PubMed: 8661500]
56. Zhou H, Lillis S, Loy RE, Ghassemi F, Rose MR, Norwood F, Mills K, Al-Sarraj S, Lane RJ, Feng L, et al. Multi-minicore disease and atypical periodic paralysis associated with novel mutations in the skeletal muscle ryanodine receptor (RYR1) gene. Neuromuscul Disord. 2010; 20:166–17. [PubMed: 20080402]
57. Al-Qusairi L, Weiss N, Toussaint A, Berbey C, Messaddeq N, Kretz C, Sanoudou D, Beggs AH, Allard B, Mandel JL, et al. T-tubule disorganization and defective excitation-contraction coupling

in muscle fibers lacking myotubularin lipid phosphatase. Proc Natl Acad Sci USA. 2009; 106:18763–1876. [PubMed: 19846786]

58. Bevilacqua JA, Bitoun M, Biancalana V, Oldfors A, Stoltenburg G, Claeys KG, Lacène E, Brochier G, Manéré L, Laforêt P, et al. Neclace fibers, a new histological marker of late onset MTM1-related centronuclear myopathy. Acta Neuropathol. 2009; 117:283–29. [PubMed: 19084976]
59. Razidlo GL, Katafiasz D, Taylor GS. Myotubularin regulates Akt-dependent survival signaling via phosphatidylinositol 3-phosphate. J Biol Chem. 2011; 286:20005–2001. [PubMed: 21478156]
60. Bers DM, Stiffel VM. Ratio of ryanodine to dihydropyridine receptors in cardiac and skeletal muscle and implications for E–C coupling. Am J Physiol. 1993; 264:C1587–C1593. [PubMed: 8333507]
61. Anderson K, Cohn AH, Meissner G. High-affinity [3H]PN200-110 and [3H]ryanodine binding to rabbit and frog skeletal muscle. Am J Physiol. 1994; 266:C462–C466. [PubMed: 8141261]
62. Margreth A, Damiani E, Tobaldin G. Ratio of dihydropyridine to ryanodine receptors in mammalian and frog twitch muscles in relation to the mechanical hypothesis of excitation-contraction coupling. Biochem Biophys Res Commun. 1993; 197:1303–131. [PubMed: 8280147]
63. Shirokova N, Garcia J, Rios E. Local Ca^{2+} release in mammalian skeletal muscle. J Physiol. 1998; 512:377–38. [PubMed: 9763628]
64. Figueroa L, Shkryl VM, Zhou J, Manno C, Marmotake A, Brum G, Blatter LA, Elli-Davies GC, Rios E. Synthetic localized calcium transients directly probe signalling mechanisms in skeletal muscle. J Physiol. 2012; 590:1389–1411. [PubMed: 22310315]
65. González A, Kirsch WG, Shirokova N, Pizarro G, Stern MD, Ríos E. The spark and its ember: separately gated local components of Ca^{2+} release in skeletal muscle. J Gen Physiol. 2000; 115:139–15. [PubMed: 10653893]
66. Peachey LD. The sarcoplasmic reticulum and transverse tubules of the frog's sartorius. J Cell Biol. 1965; 25:209–231. [PubMed: 5840799]
67. Drummond GI, Hanvood JP, Powell CA. Studies on the activation of phosphorylase in skeletal muscle by contraction and by epinephrine. J Biol Chem. 1969; 244:4235–4240. [PubMed: 4308172]
68. Entman ML, Keslensky SS, Chu A, Van Winkle WB. The sarcoplasmic reticulum-glycogenolytic complex in mammalian fast twitch skeletal muscle. Proposed *in vitro* counterpart of the contraction-activated glycogenolytic pool. J Biol Chem. 1980; 255:6245–6252. [PubMed: 6446555]
69. Katz A, Andersson DC, Yu J, Norman B, Sandstrom ME, Wieringa B, Westerblad H. Contraction-mediated glycogenolysis in mouse skeletal muscle lacking creatine kinase: the role of phosphorylase b activation. J Physiol. 2003; 553:523–53. [PubMed: 12963789]
70. Hellstein Y, Richter EA, Kiens B, Bangsbo J. AMP deamination and purine exchange in human skeletal muscle during and after intense exercise. J Physiol. 1999; 520:909–92. [PubMed: 10545153]
71. Allen DG, Lamb GD, Westerblad H. Impaired calcium release during fatigue. J Appl Physiol. 2007; 104:296–30. [PubMed: 17962573]
72. Stephenson DG. In pursuit of the glycogen [Ca^{2+}] connection. J Physiol. 2011; 589:451. [PubMed: 21285024]
73. Ortenblad N, Nielsen J, Saltin B, Holmberg HC. Role of glycogen availability in sarcoplasmic reticulum Ca^{2+} kinetics in human skeletal muscle. J Physiol. 2011; 589:711–72. [PubMed: 21135051]

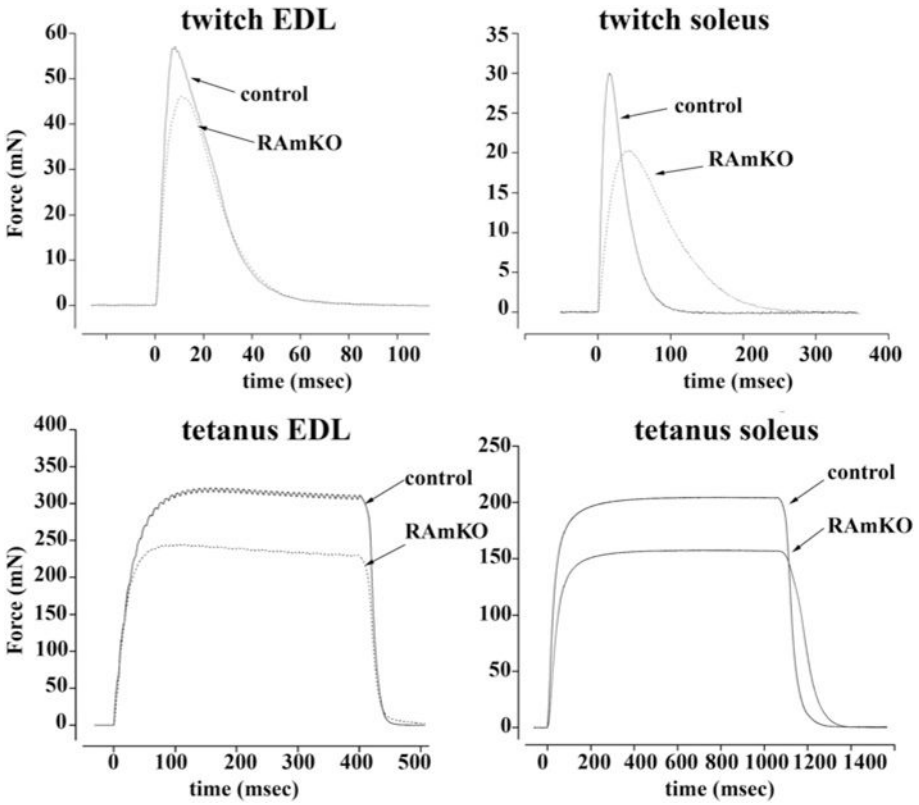

Figure 1. Mechanical properties of isolated EDL and soleus muscles from RamKO and control littermates

Isolated muscles from 8-week-old mice were electrically stimulated as described in the 'Materials and Methods' section. Top panels show single twitches, bottom panels maximal tetanus force. Dotted line RamKO mice, continuous line control littermates. Note that the muscles from RamKO mice developed approximately 20% less force than controls. Slow twitch muscles also showed a significant decrease in the half relaxation time. Traces are representative of experiments carried out by Bentzinger et al. [12] on at least three/four different muscle preparations.

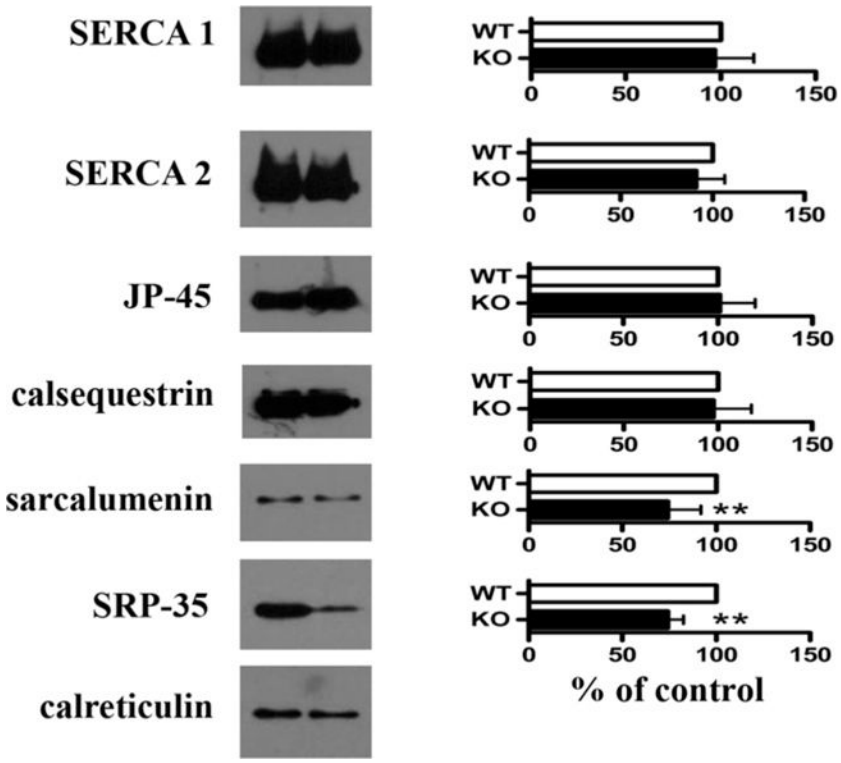

Figure 2. Biochemical characterization of SR proteins from RamKO mice

Left panels show representative Western blots with specified Abs; right panels, mean band intensity (± S.D.) of 6–9 determinations from three different SR preparations. Values were normalized with respect to intensity values obtained from control littermates. White bars, controls; black bars, RamKO. ** $P < 0.002$.

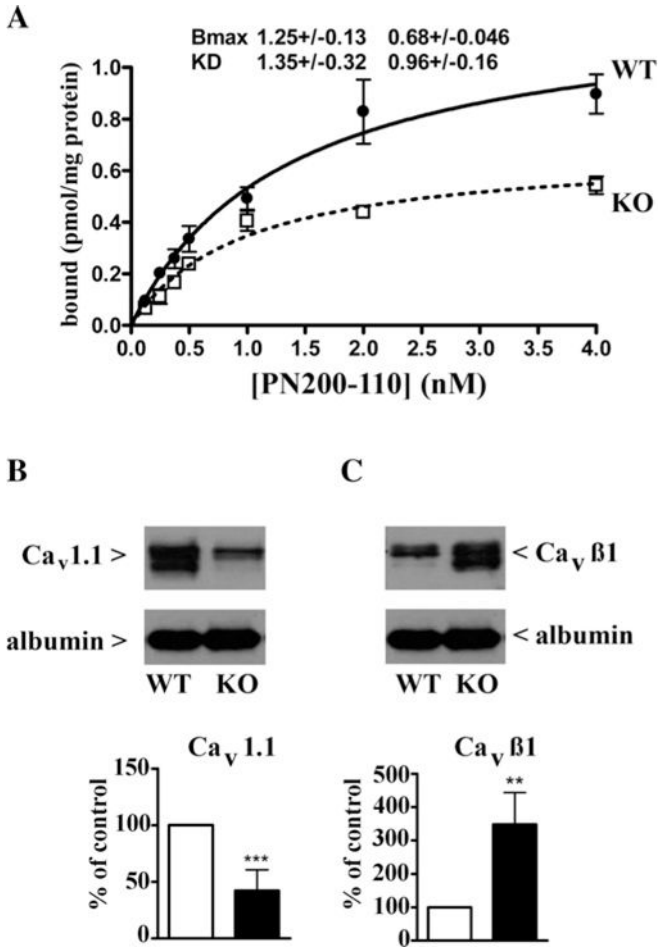

Figure 3. $Ca_V1.1$ is decreased in RamKO mice

(**A**) Equilibrium binding of PN200-110 to skeletal muscle SR of control (filled circle) and RamKO (empty boxes) mice. Data points represent mean (± S.E.M.) of six determinations carried out in two different SR preparations. (**B** and **C**) Western-blots of Ca_V 1.1 and Ca_V β1 in SR of control (empty bars) and RamKO (filled bars) mice; the mean band intensity of 5–7 determinations from three different SR preparations.

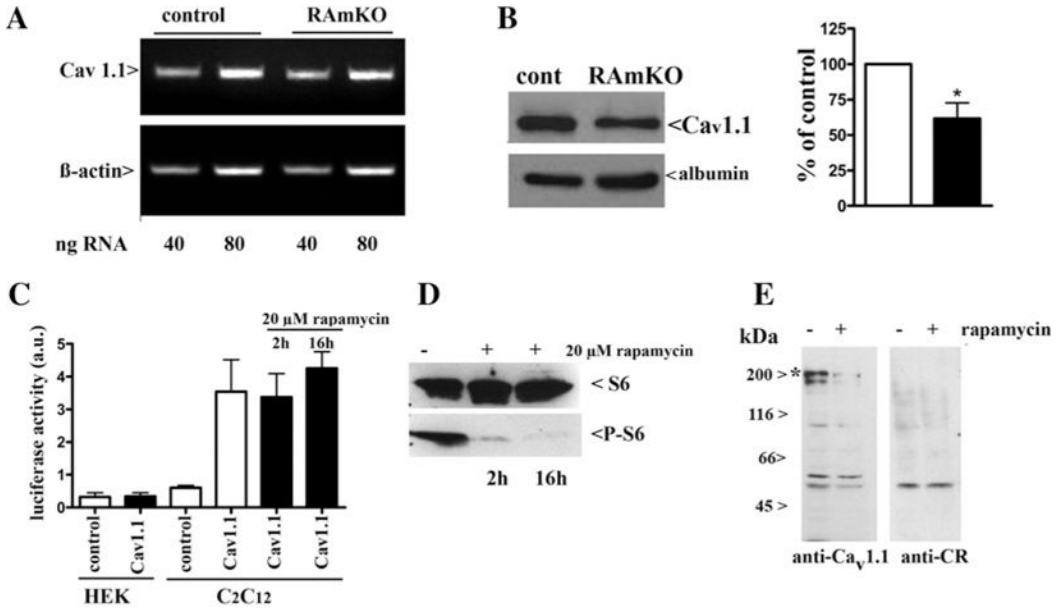

Figure 4. $Ca_v1.1$ decrease in RamKO mice is not due to a decrease in transcription of $Ca_v1.1$ mRNA

(**A**) Semi-quantitative RT–PCR of $Ca_v1.1$. The Figure represents results obtained in four different experiments with RNA extracted from two muscle preparations. (**B**) Western blot of total muscle homogenate with anti-$Ca_v1.1$ and anti-albumin, a marker for transverse tubule content. The bar histogram shows mean (± S.E.M.) band intensity of six determinations from four different muscle preparations; band intensity from the RamKO mice are normalized to that obtained in control littermates. (**C**) The $Ca_v1.1$ promoter is not affected by treatment with 20 μM rapamycin as determined by luciferase activity. No activity was seen upon transfection of cells with either a control plasmid (white bars) or upon transfection of HEK293 with the luciferase reporter (black bars). C_2C_{12} cells transfected with a control plasmid showed no luciferase activity, whereas transfection with the luciferase reporter resulted in strong activity which was not affected by 2 or 16 h incubation with rapamycin (black bars). (**D**) Rapamycin treatment of C_2C_{12} cells was effective as it resulted in the decrease in phosphorylation of S6 after 2 and 16 h. (**E**) Rapamycin treatment of differentiated C_2C_{12} causes a decrease in $Ca_V1.1$ as determined by Western blotting. Cells were treated with 20 μM rapamycin for 16 h and 25 μg of microsomes were loaded on SDS/7.5% PAGE and blotted on to nitrocellulose. The blot was probed with anti-$Ca_V1.1$, stripped and re-probed with anti-CR Ab as a loading control; *band corresponding to the $Ca_V1.1$ protein.

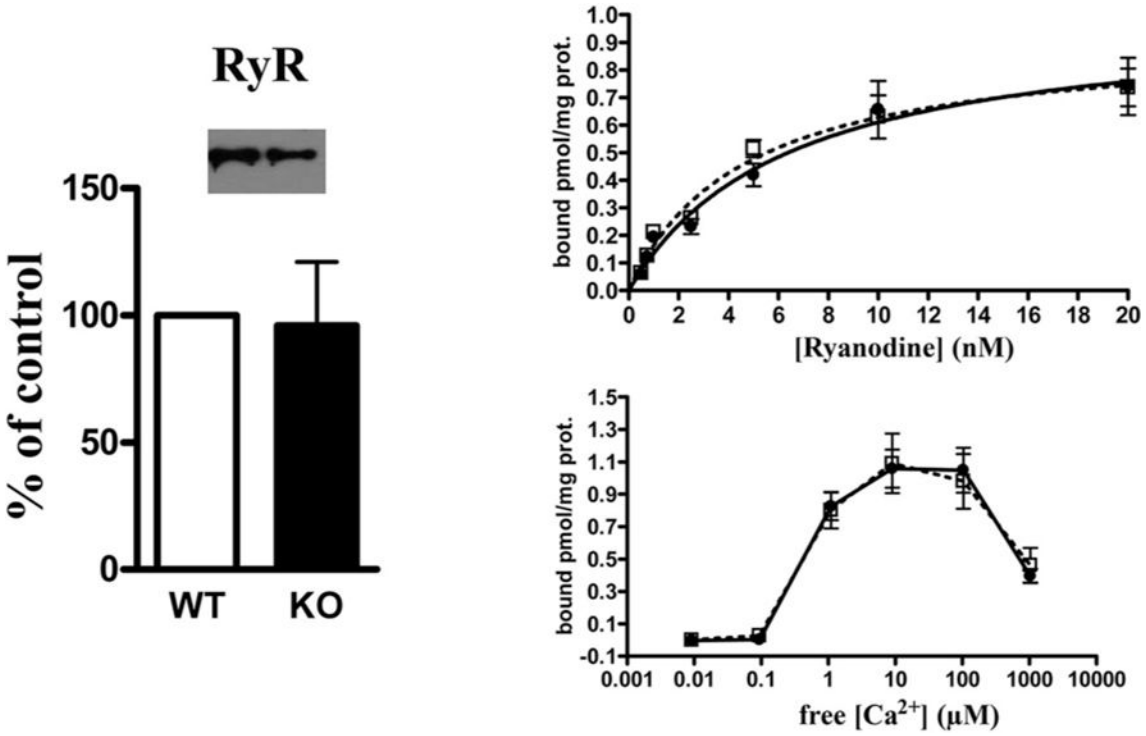

Figure 5. RyR content and functional characteristics are not changed in RamKO mice

Left panel: Representative Western blot of total SR and mean band intensities (± S.D.) of eight determinations from three different SR preparations. Top right: [^{3}H]ryanodine binding to SR preparations from control (filled circles) and RamKO (open boxes) mice were performed as described in the 'Materials and Methods'. Data points represent the mean (± S.E.M.) of 12 determinations from three different SR preparations. No significant change in the B_{max} or apparent K_D was found. Bottom right: Ca^{2+} -dependent [^{3}H]ryanodine binding to SR preparations from control (filled circles) and RamKO (open boxes) mice. Data points represent mean (± S.E.M.) of six determinations on two different SR preparations.

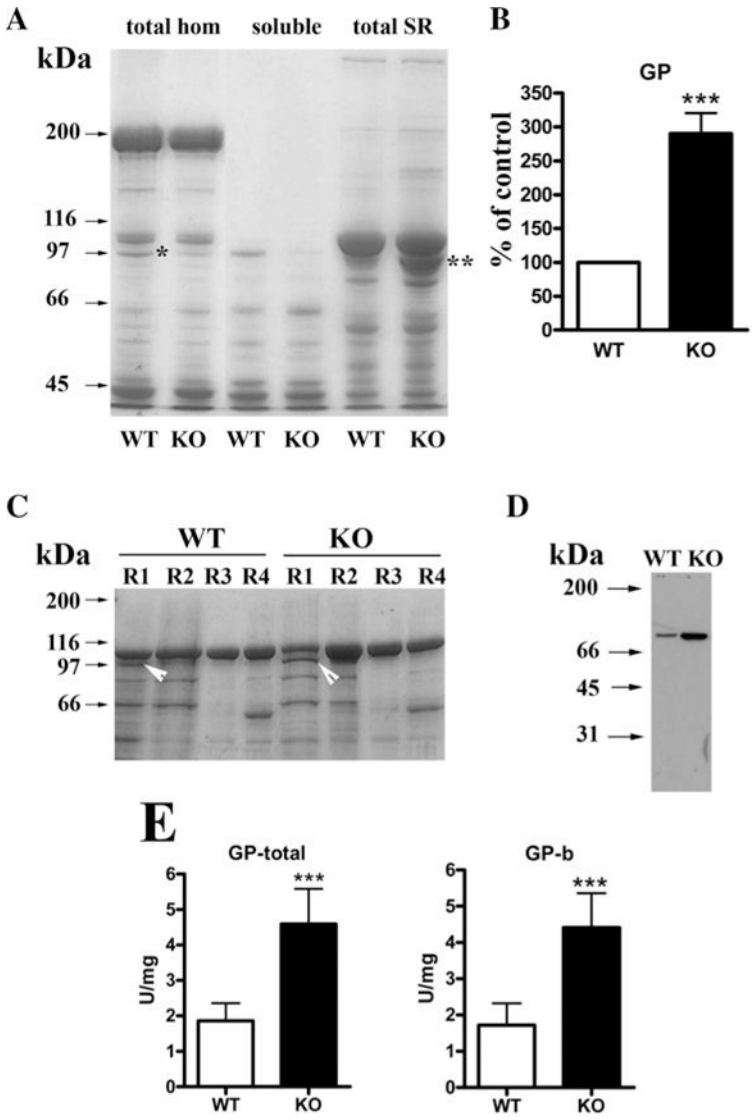

Figure 6. GP is accumulated in the SR of RamKO mice and represents mainly the enzymatically-inactive form

(**A**) Ten μg of protein from total skeletal muscle homogenate, myoplasm or SR fraction was separated on a SDS/7.5% PAGE and stained with SimplyBlue Safe Stain. *Represents a band present in the total homogenate from WT muscle but not in RamKO muscle; **represents a band present in the SR fraction of RamKO mice but not in WT mice. (**B**) Densitometric analysis of GP band in total SR of control (white bars) and RamKO (black bar) mice. (**C**) SR was fractioned into light SR (R1), longitudinal SR (R2) and terminal cisternae (R4). Fifteen μg of protein from each fraction was loaded on a SDS/7.5% PAGE and stained with SimplyBlue Safe Stain or (**D**) blotted on to nitrocellulose and stained with anti-GP Abs. White arrows in C indicate GP, which is enriched in the light SR fraction R1. (**E**) Total (left bar histogram) and inactive form (right bar histogram) GP enzymatic activity in SR from control (white bars) and RamKO (black bars) mice. Values represent the mean (± S.D.) of 11 determinations from three different SR preparations. ***$P < 0.05$.

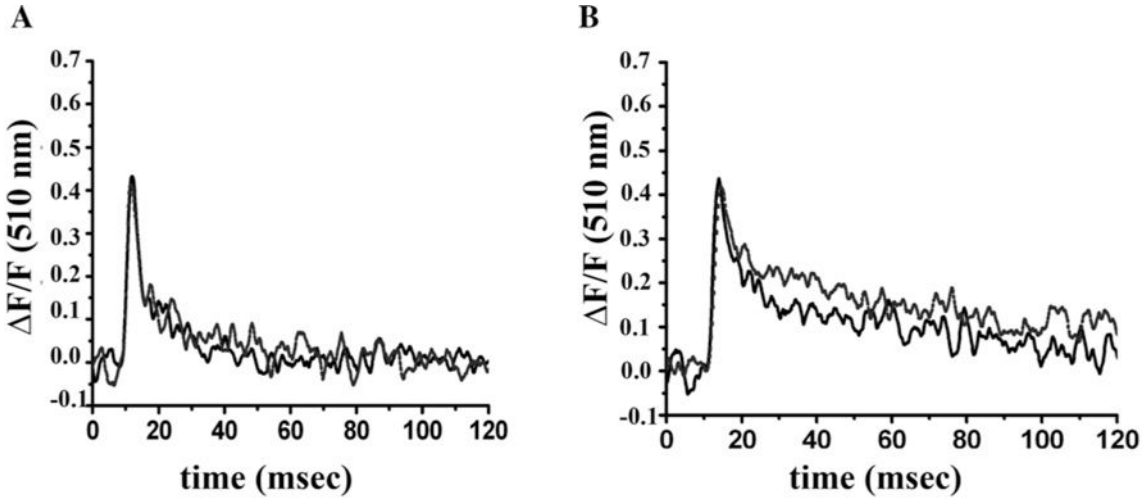

Figure 7. Changes in the myoplasmic [Ca^{2+}] of individual, enzymatically dissociated EDL and soleus fibres

Control and RamKO fibres were loaded with 10 μM mag–fluo–4AM in Tyrode's solution for 10–15 min at 20°C. This solution was replaced and acquisitions were made during continuous perfusion with Tyrode's buffer plus 50 μM BTS. Calcium transients were elicited by single pulses of 1 ms duration, through a platinum electrode inside a glass pipette placed near the fibre surface. The representative traces from EDL (**A**) and soleus (**B**) show no differences in the peaks and velocities of the Ca^{2+} transients; there is a significant increase in the half relaxation time in soleus fibres from RamKO mice. See Table 1 for a thorough analysis of the kinetic parameters.

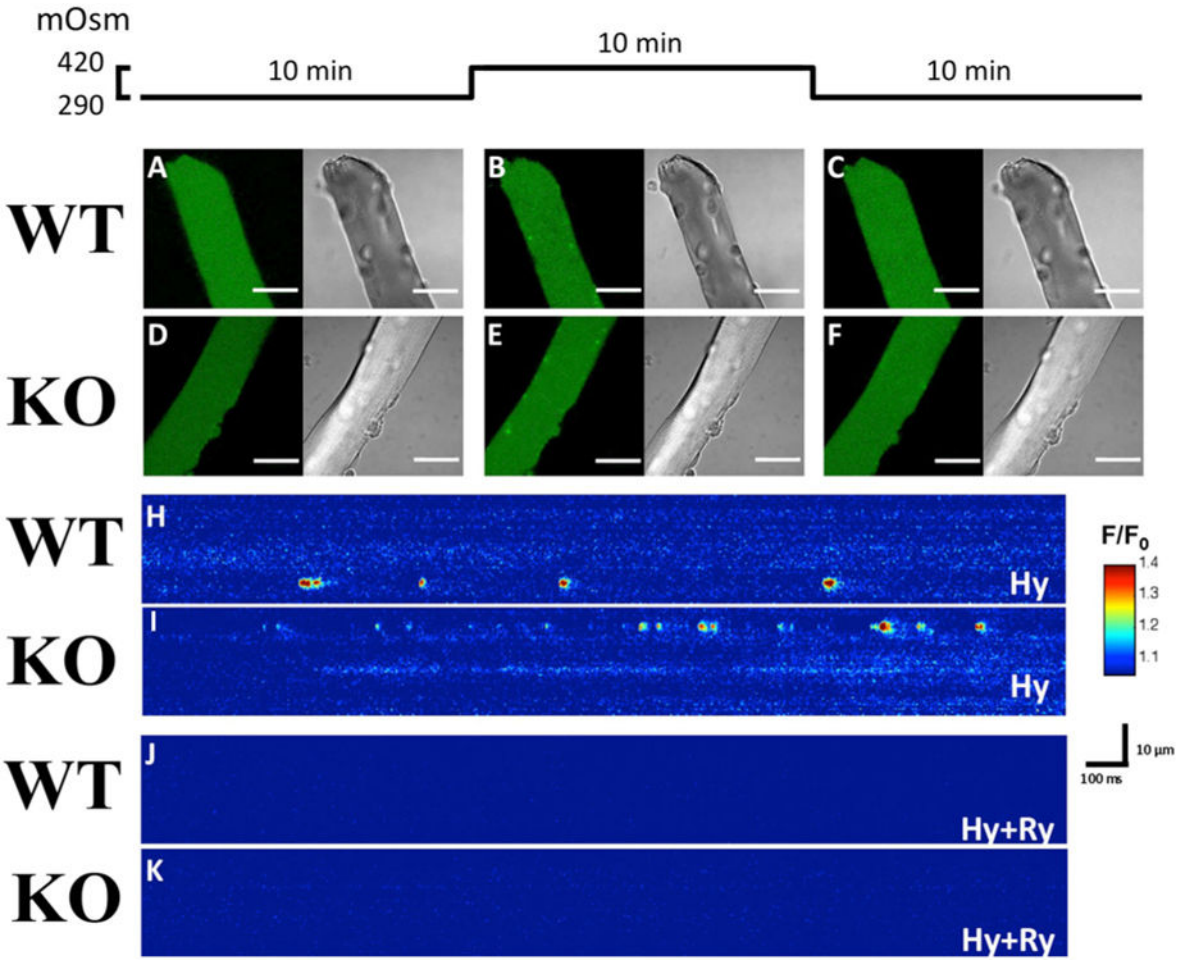

Figure 8. Osmotic-shock triggered ECRE are more frequent in FDB fibres from RamKO than WT mice

ECREs were triggered by exposure of FDB fibres to a hyperosmotic solution. (**A**–**F**) Left images show fluo–4 fluorescence and right images bright-field images of the same FDB fibre. Scales bars = 30 μm. (**A** and **D**) show (*xy*) images of the calcium fluorescence (AU) in WT and RamKO fibres in NR, (**B** and **E**) show images of the same fibres after hyperosmotic shock treatment and (**C** and **F**) show images of the fibres after 10 min re-perfusion with a normo-osmotic Ringer solution; as shown after removal of the hyperosmotic medium ECRE are no longer visible. (**H** and **I**) are pseudocoloured linescan images (*xt*) showing in detail the ECREs shape in WT and RamKO fibres when bathed with hypertonic solution (Hy). (**J** and **K**) show that ECREs are due to the opening of RyRs as they are abolished by a 30 min pre- incubation with 10 μM. Scale bar (**H**–**K**): horizontal: 100 ms, vertical: 10 μm.

Table 1

Kinetic properties of calcium transients of isolated EDL and soleus fibres from control and RamKO mice

	Resting Ca^{2+} [nM]†	Peak amplitude‡ (Δ*F*/*F*)	Time to peak (ms)	Rise time 10%–90% (ms)	Fall time 10%–90% (ms)
EDL control	141.0 ± 0.35 (*n*= 23)	0.46 ± 0.04 (*n*= 29)	2.9 ± 0.1 (*n*= 29)	1.7 ± 0.05 (*n*= 29)	34.1 ± 4.3 (*n*= 29)
EDL RAmKO	115.5 ± 4.8 * (*n*= 21)	0.43 ± 0.02 (*n*= 27)	3 ± 0.1 (*n*= 27)	1.8 ± 0.06 (*n*= 27)	39.4 ± 5.4 (*n*= 27)
Soleus control	117 ± 3.6 (*n*= 26)	0.38 ± 0.02 (*n*= 22)	3.4 ± 0.2 (*n*= 22)	2.1 ± 0.2 (*n*= 22)	66.2 ± 7.4 (*n*= 22)
Soleus RamKO	93.8 ± 4.26 * (*n*= 8)	0.36 ± 0.02 (*n*= 25)	3.4 ± 0.1 (*n*= 25)	2.1 ± 0.1 (*n*= 25)	120.3 ± 15.7 * (*n*= 25)

Values are mean ± S.E.M.; n, number of fibres from six WT and RamKO mice.

* *P*< 0.05 Mann Whitney U test.

‡† Calcium measurements performed with the ratiometric indicator indo-1.

‡ Calcium measurements performed with mag–fluo–4.

Table 2

Morphology of ECREs in skeletal muscle fibres

		Amplitude ($\Delta F/F_0$)	FWHM (μm)	FDHM (ms)	Mass	Freq* (Sparks/image)	N†
<50 ms ECREs	WT	0.38 ± 0.00	0.89 ± 0.01	13.31 ± 0.26	0.62 ± 0.02	6.81 ± 0.36	1923
	RamKO	0.38 ± 0.00	0.98 ± 0.01‡	14.11 ± 0.24‡	0.85 ± 0.03‡	8.83 ± 0.40‡	2547
>50 ms ECREs	WT	0.56 ± 0.01	1.32 ± 0.02	143.36 ± 3.32	2.51 ± 0.17	2.51 ± 0.17	538
	RamKO	0.60 ± 0.01‡	1.45 ± 0.02‡	138.49 ± 2.80	3.56 ± 0.18‡	3.56 ± 0.18‡	731

Values are expressed as mean ± S.E.M.

*WT 168 images, RamKO 162 images.

†Number of ECREs analysed in 25 fibres and 26 fibres from five WT and RamKO five mice respctively.

‡$p<0.005$ Student t test.